Sleep and wake modulate spine turnover in the adolescent mouse cortex

Stephanie Maret[1,3], Ugo Faraguna[1,3], Aaron B Nelson[2,3], Chiara Cirelli*[,3], and Giulio Tononi*[, 3]

1, both authors contributed equally
2, Neuroscience Training Program, University of Wisconsin-Madison
3, Department of Psychiatry, University of Wisconsin/Madison, Wisconsin, U.S.A.

*Corresponding authors:
Chiara Cirelli
Giulio Tononi

University of Wisconsin/Madison
Department of Psychiatry
6001 Research Park Blvd
Madison WI 53719
Tel. (608) 263 9236
Fax. (608) 263 9340
ccirelli@wisc.edu
gtononi@wisc.edu

Abbreviated title: Sleep and synaptic pruning
1 figure, 3 supplementary figures
Keywords: sleep, cortex, synapse, adolescence, pruning

Acknowledgements. The study was supported by NIH Director's Pioneer award (to GT) and NIMH (1R01MH091326 to GT and CC).

Supplementary Discussion

It should be emphasized that, despite the net gain of synapses after wake and the net loss after sleep, individual spines could form and retract irrespective of the predominant behavioral state between the two imaging sessions. On the other hand, mice were never spontaneously asleep or awake for many hours without cycling at least briefly to another behavioral state, a fact that may have contributed to the presence of both spine loss and spine gain in each experimental group. Regardless, W1SD2 mice never slept between the two imaging sessions, and yet they showed some spine loss. It is possible that long episodes of wake or sleep occurring prior to the time points evaluated in the current analysis may also be responsible for some confounding effects on synaptic changes.

We also found that spine formation was significantly higher after several hours of (mostly) wake than after several hours of (mostly) sleep (Fig. 1d). This suggests that although wake-related, experience-driven activity is not an absolute requirement for spinogenesis, it nonetheless promotes it. On the other hand, we found a clear trend towards greater spine loss after long sleep than after long spontaneous wake, but the difference did not reach significance. Thus, based on these data we cannot establish conclusively whether the *net* spine loss observed after sleep is due to an active process of spine elimination directly promoted by sleep, or is the consequence of suboptimal conditions for spine formation during sleep, or both. We have suggested[1] that there are several mechanisms by which sleep could bring about a net decrease in synaptic strength, including 1) the occurrence during NREM sleep of repeated sequences of depolarization / synchronous firing (up state) and hyperpolarization / silence (down state) at ~ 1 Hz; 2) the presence of low levels of neuromodulators such as noradrenaline, serotonin, hypocretin and histamine; 3) the low expression of BDNF. In vitro studies suggest that the first mechanism may actively promote synaptic depression by facilitating the endocytosis of AMPA receptors [2], while the other two mechanisms may more directly prevent synaptic potentiation rather than actively promote synaptic depression[3, 4]. Thus, it is currently unclear to what extent the role of sleep in spine elimination is permissive and/or instructive.

Supplementary Figures and Methods

Supplementary Figure 1

Sleep duration data from eight ~ P30 mice are represented. Each plot displays the duration of total sleep (min/hr) as determined by EEG visual scoring (circles) or by video-based motion detection (triangles). The dark period is indicated by black horizontal bars. For each animal the concordance value between EEG-based and video-based scoring is indicated. EEG-based behavioral states were scored in 4-sec epochs, while the video-based motion detection resolution was 1 sec. For the concordance analysis a minimum duration criterion was applied, which defines sleep as any period of immobility ≥ 40 sec. This criterion has been validated in our lab and in a previous study[5].

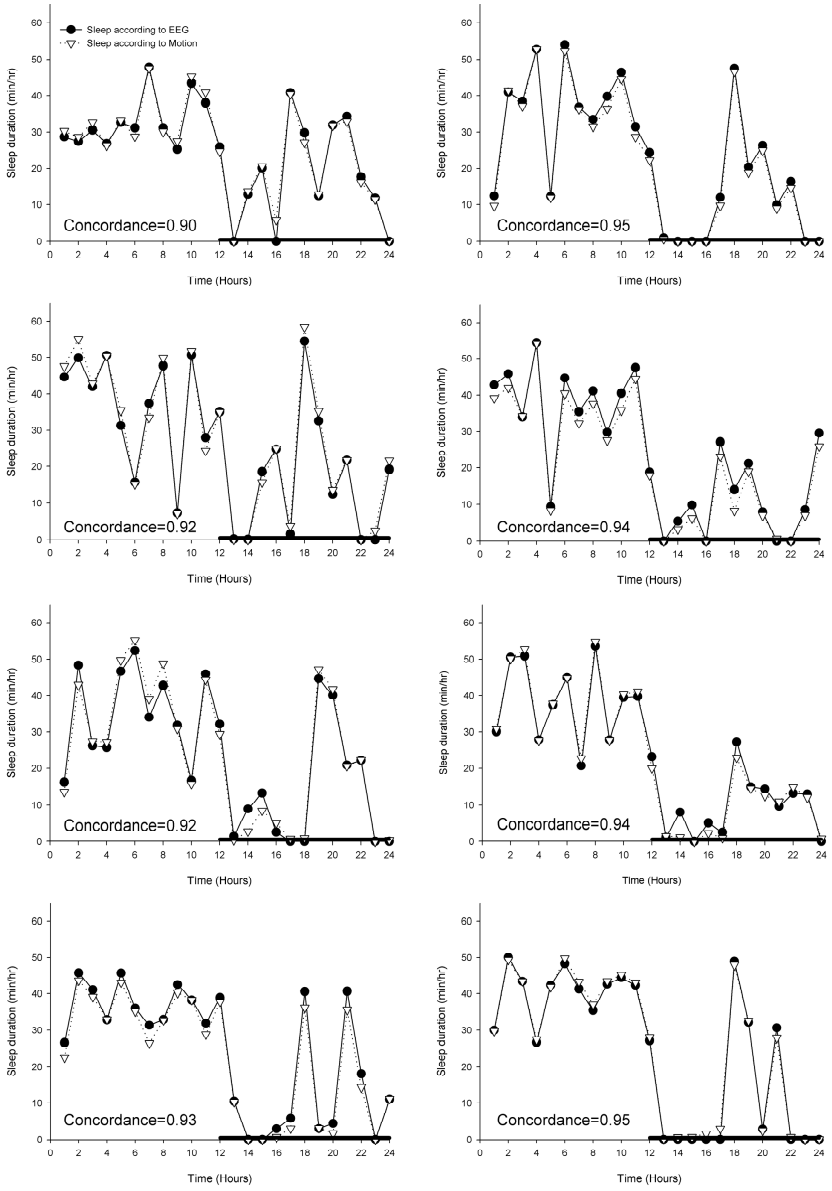

Supplementary Figure 2
Net spine changes in each individual adolescent mouse for the "wake" (S1W2+W1SD2, A) and "sleep" (W1S2, B) groups, plotted against postnatal age.

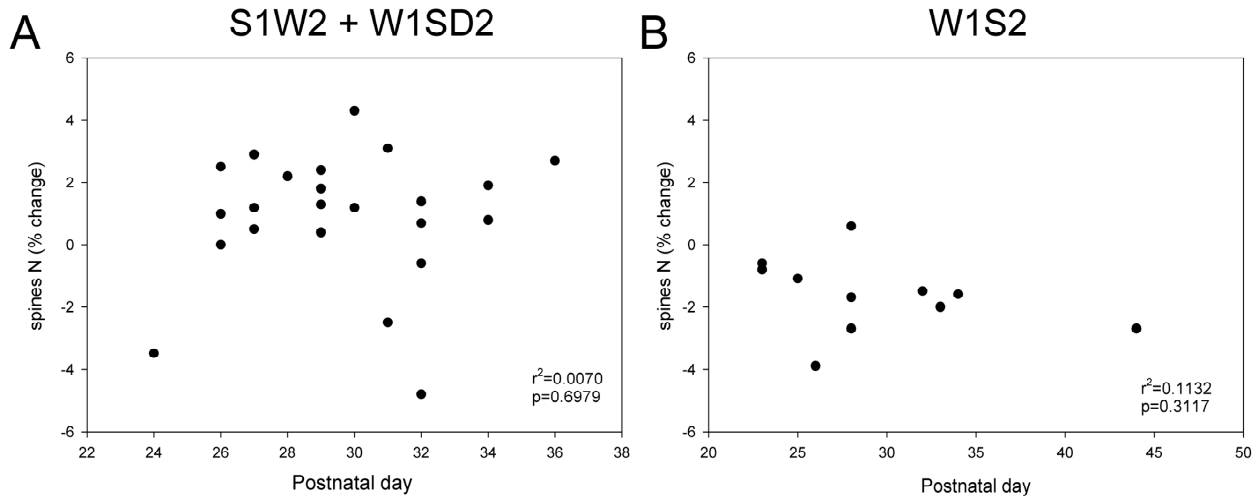

Supplementary Figure 3
Net spine changes depending on sleep and wake duration in adolescent mice.

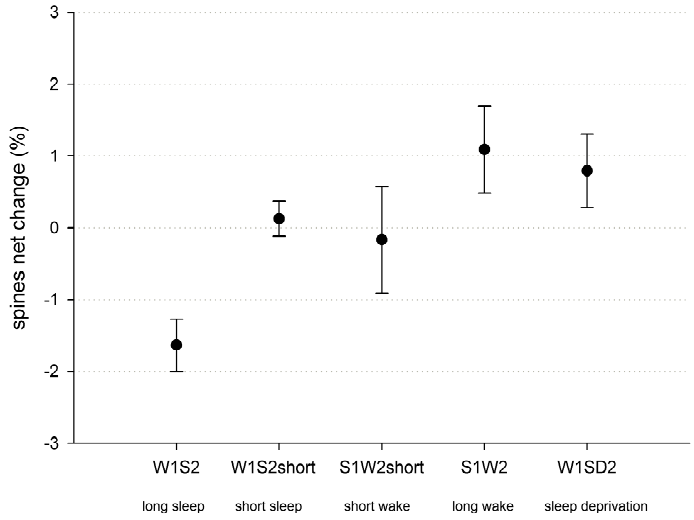

Recordings of sleep and locomotor activity

Yellow fluorescent protein (YFP)-H-expressing mice[6] (Jackson Laboratory, Bar Harbor, Maine) were housed individually and maintained on a 12 hrs light / 12 hrs dark cycle (lights on at 8am) with food and water available *ad libitum*. Sleep was recorded using standard electroencephalogram (EEG) recordings as in previous reports[7, 8]. Briefly, prior to surgery, all electrodes were directly soldered to flexible wires (#NUF30-4046, Cooner Wire, Chatsworth, CA). Mice (P20-P40) were anesthetized with isoflurane (~1.4% in 100% O_2) and gold plated miniature screw electrodes (0.7mm diameter) were placed over right and left frontal (anteroposterior, AP, +1 mm from bregma; mediolateral, ML, 1 mm), and parietal (AP −2 mm; ML 2 mm) cortices and one over cerebellum as reference. Two vinyl-coated braided stainless steel wire electrodes (#AS636, Cooner Wire) were placed in the nuchal muscle for electromyogram (EMG) recording. Electrodes were insulated and affixed to the skull using dental cement. Following surgery, mice were housed individually in sound-attenuating, environmentally controlled recording chambers (12:12 LD, lights on at 8am, 25ºC ± 1°C, food and water *ad libitum*). All electrodes were gathered into a flexible cable and connected to the Multichannel Neurophysiology Recording system (Tucker-Davis Technologies, TDT, Alachua, FL). EEG and EMG signals were collected continuously at a sampling rate of 256 Hz (digitally filtered between 0.1-100 Hz). For sleep staging, signals were processed by custom-made Matlab scripts (Mathworks, Natick, MA) using standard TDT routines and subsequently converted into European Data Format (EDF) with Neurotraces software (www.neurotraces.com, Fort Lauderdale, FL). Twenty-four hour polygraphic recordings were scored offline for NREM sleep, REM sleep, and wake by visual inspection of 4-sec epochs (SleepSign; Kissei Comtec, Irvine, CA) according to standard criteria. Wake was characterized by low voltage, high frequency EEG pattern and phasic EMG activity. NREM sleep was characterized by the occurrence of high amplitude slow waves and low tonic EMG. During REM sleep the EEG was similar to that during wake, but only heart beats and occasional twitches were evident in the EMG signal. EEG power spectra of consecutive 4-sec epochs (FFT routine, Hanning window) were calculated for the fronto-cerebellar derivations within the frequency range of 0.1-30 Hz.

Motor activity was quantified by custom-made video-based motion detection algorithms with a time resolution of 1 sec (Matlab). Since time spent asleep could be reliably estimated using motion detection (93 $\pm$ 2.0 % concordance with EEG, n=8 Supplementary Fig. 1), mice used for two-photon imaging were monitored using video cameras and direct visual observation, to reduce skull damage and risk of inflammation due to implant of EEG electrodes. The latter is a crucial issue, because acute inflammation may affect spine dynamics[9].

All animal procedures followed the National Institutes of Health Guide for the Care and Use of Laboratory Animals and facilities were reviewed and approved by the IACUC of the University of Wisconsin-Madison, and were inspected and accredited by AAALAC.

Skull thinning for two-photon laser scanning microscopy

Training for skull thinning was done under the direct supervision of Dr. Yi Zuo and her student Xinzhu Yu (University of California Santa Cruz) and performed essentially as described in [10]. YFP-H mice were anesthetized with isoflurane (~1.4% in 100% O_2) and the skull above barrel cortex was exposed, cleaned, and thinned to ~ 50% of its original thickness using a high-speed drill (Fine Science Tools, Belmont, CA). Drilling was intermittent and a cold sterile solution was periodically applied to the skull to reduce heat-induced cortical damage. Skull thinning was completed (final bone layer = ~20-40 μm) using a microsurgical blade (#6900, Surgistar, Vista, CA). To reduce movement artifacts due to breathing the skull was glued to a ~ 400 μm thick stainless steel plate

with a central opening for skull access and the plate was screwed on both sides to a metal base attached to the microscope. After the first imaging the plate was detached from the skull and the scalp was sutured until the second imaging session.

In vivo imaging of dendritic protrusions

Transcranial imaging was performed under isoflurane anesthesia (~1.4% in 100% O_2) using a two-photon microscope (Prairie Technologies, Madison, WI) with a Ti:Sapphire laser (Cameleon Coherent, Coherent Inc., Santa Clara, CA) tuned to the excitation wavelength for YFP (920 nm). Low laser power (< 20 mW at the sample) was used to decrease the risk of phototoxicity, and mice with any signs of photodamage after the first session were discarded. Utmost care was devoted to selecting only those animals in which the quality of the repeated imaging sessions was comparable. Stacks of image planes were acquired using a water-immersion 60X objective zoom (Olympus, LUMPlanFI/IR, 0.8 numerical aperture; 3X optical zoom). Dendritic branches were imaged at ~50 to ~200 μm from the pial surface and the step size was 0.70 μm. Two-dimentional projections of three-dimentional image stacks were used for Figure 1.

Data quantification

The same dendritic segments (5-25 μm in length) were imaged twice within ~ 12-16 hours. The unique vascular pattern of the thinned region was used to grossly position the objective to within ~ 150 μm of the region of interest. YFP fluorescence imaging was then used to identify specific dendritic segments based on their unique branching pattern. Previous studies of YFP-H mice[10, 11] have shown that these randomly chosen segments are likely from different parent neurons, due to the high density of labeled cells in this mouse strain. All dendritic protrusions clearly (5 pixels = 0.65 μm) emanating laterally from the dendritic shaft were classified as spines or filopodia (long and thin protrusions without a bulbous head[10]) and analyzed separately. Spines were classified into classes (stubby, thin, mushroom) based on length, spine head diameter, and neck diameter [12]. All analyses were done blind, with the analyzer unaware of experimental condition (i.e. experimental group and imaging session). The identification of the spines used for analysis was performed visually. NeuronStudio (CNIC, Mount Sinai School of Medicine) was used to archive the detection and classification of manually detected spines[13].

Experimental groups

Each animal was imaged twice within 12-16 hours, and all mice were selected based on the sleep/wake pattern during the 8-12 hours that preceded each imaging session. A first group of animals (W1S2, n = 11; Fig. 1b) was imaged shortly after light onset, after they had been spontaneously awake for at least 75% of the time in the previous 12-hour dark period; during the last 1-2 hours mice were given novel objects and access to a running wheel, to avoid the occurrence of any intervening sleep immediately before the first imaging session, and to standardize the wake condition across all animals. After the first imaging session mice were left undisturbed and spent the following 6-8 hours mainly asleep (>65% of total time) before being imaged a second time. A second group of animals (S1W2, n = 11; Fig. 1b) was asleep for at least 65% of the time in the previous 8-12 hrs during the light period, imaged, and then remained awake for most of the following 10-12 hours (>85% of total time). As in the first group, mice were exposed to novel objects and a running wheel in the last 1-2 hours, around light onset, to standardize their wake before the second imaging session. In the third group of mice spontaneous wake at night was followed by 6-7 hours of forced wake maintained by exposure to a running wheel and novel objects

(W1SD2, n=13; Fig. 1b). Thus, in these mice the second imaging session occurred at the end of the light phase, at the same time of day as for the W1S2 group, but after a prolonged period of wake rather than sleep. All mice used for imaging had previously been habituated to novel objects and running wheels by brief daily exposure to these items. Overall, ~80% of the mice that met the behavioral criteria for sleep/wake had a successful first imaging session. Of those, ~60-70% met the behavioral criteria for the second imaging session and were imaged. Of those, only 40-50% were selected based on the quality of the second imaging session (no tissue damage, orientation matched that for the first imaging session, etc) and included in the study.

1. Tononi, G. & Cirelli, C. Sleep function and synaptic homeostasis. *Sleep Med Rev* **10**, 49-62 (2006).
2. Lante, F., Toledo-Salas, J.C., Ondrejcak, T., Rowan, M.J. & Ulrich, D. Removal of synaptic Ca(2)+-permeable AMPA receptors during sleep. *J Neurosci* **31**, 3953-3961 (2011).
3. Seol, G.H.*, et al.* Neuromodulators control the polarity of spike-timing-dependent synaptic plasticity. *Neuron* **55**, 919-929 (2007).
4. Jiang, B., Akaneya, Y., Hata, Y. & Tsumoto, T. Long-term depression is not induced by low-frequency stimulation in rat visual cortex in vivo: a possible preventing role of endogenous brain-derived neurotrophic factor. *J Neurosci* **23**, 3761-3770 (2003).
5. Pack, A.I.*, et al.* Novel method for high-throughput phenotyping of sleep in mice. *Physiol Genomics* **28**, 232-238 (2007).
6. Feng, G.*, et al.* Imaging neuronal subsets in transgenic mice expressing multiple spectral variants of GFP. *Neuron* **28**, 41-51 (2000).
7. Douglas, C.L.*, et al.* Sleep in Kcna2 knockout mice. *BMC Biol* **5**, 42 (2007).
8. Vyazovskiy, V.V., Cirelli, C., Pfister-Genskow, M., Faraguna, U. & Tononi, G. Molecular and electrophysiological evidence for net synaptic potentiation in wake and depression in sleep. *Nat Neurosci* **11**, 200-208 (2008).
9. Bhatt, D.H., Zhang, S. & Gan, W.B. Dendritic spine dynamics. *Annu Rev Physiol* **71**, 261-282 (2009).
10. Grutzendler, J., Kasthuri, N. & Gan, W.B. Long-term dendritic spine stability in the adult cortex. *Nature* **420**, 812-816 (2002).
11. Xu, T.*, et al.* Rapid formation and selective stabilization of synapses for enduring motor memories. *Nature* **462**, 915-919 (2009).
12. Peters, A. & Kaiserman-Abramof, I.R. The small pyramidal neuron of the rat cerebral cortex. The perikaryon, dendrites and spines. *Am J Anat* **127**, 321-355 (1970).
13. Rodriguez, A., Ehlenberger, D.B., Dickstein, D.L., Hof, P.R. & Wearne, S.L. Automated three-dimensional detection and shape classification of dendritic spines from fluorescence microscopy images. *PLoS ONE* **3**, e1997 (2008).